

LONG-TIME EVOLUTION OF THE INCOMPRESSIBLE THREE-DIMENSIONAL TAYLOR-GREEN VORTEX AT VERY HIGH REYNOLDS NUMBER

Felix S. Schraner

Institute of Aerodynamicss
Technische Universität München
Garching, Germany
felix.schraner@aer.mw.tum.de

Xiangyu Hu

Institute of Aerodynamics
Technische Universität München
Garching, Germany
xiangyu.hu@tum.de

Nikolaus A. Adams

Institute of Aerodynamics
Technische Universität München
Garching, Germany
Nikolaus.Adams@tum.de

ABSTRACT

For this study a spatially high-order, shock capturing non-oscillatory finite volume method is combined with a weakly compressible flow modeling. As an alternative to methods based on the incompressibility assumption this weakly compressible high-resolution approach is both robust to underresolution and spatially highly accurate. The implicit subgrid-scale (SGS) model permits physically consistent underresolved simulations of incompressible, isotropic turbulent flows at very high Reynolds numbers.

Underresolved three-dimensional Taylor-Green vortex (TGV) simulations at finite Reynolds numbers are compared to reference data. Hereby, direct numerical simulation (DNS) data for $Re \leq 3000$ is used to assess the accuracy and physical consistency. Large eddy simulation (LES) predictions with two explicit as well as one implicit SGS model help to benchmark the SGS modeling capabilities. The weakly compressible high-resolution approach gives most accurate predictions for the viscous TGV even when resolution is very low. In contrast to the LES our implicit LES predict the laminar-turbulent transition physically consistently. The dissipation rates compare to those of the reference implicit LES, however, at much lower computational costs and mathematical complexity.

As our weakly compressible high-resolution approach is designed for the physically consistent simulation of very high Re turbulent flows, an infinite Re TGV is studied for an extended period of time. Thereby, the evolution at times beyond the obviously temporary quasi-isotropic state are of particular interest. For the high and infinite Re TGV flows, transition to the isotropic state is observed. Its onset and end are identifiable from a macroscopic energy redistribution within the low-modes. Subsequently, the inertial subrange scales according to $E(k) \propto k^{-5/3}$ and is self-similar in time.

1 Introduction

The three-dimensional Taylor-Green vortex (TGV) G. I. Taylor (1937) is the most simple generic flow to study the generation and evolution of small scale turbulent structures by vortex stretching and the evolution of isotropic turbulence in time. Brachet *et al.* M.E. Brachet (1984) have investigated the transitioning, viscous TGV with direct numerical simulation (DNS) resolving the entire interacting range of wavenumbers.

Numerical simulations of high Reynolds number turbulent flows are out of reach for DNS. Explicit large eddy simulations (LES) can significantly decrease computational costs. The Smagorinsky model of J. Smagorinsky (1963) and the dynamic Smagorinsky model of Sagaut (2005) are most popular for closure of the subgrid scale (SGS) stress term. The nonlinear regularization mechanism of high-order finite-volume schemes with shock-capturing capabilities can be used for implicit LES, for a review refer to Grinstein *et al.* (2007). A spectral extension of modified differential equation analysis (MDEA), see ref. Margolin & Rider (2002), has allowed to design the truncation error of a nonlinear scheme such that it recovers the theoretical spectral eddy viscosity when the flow is turbulent and underresolved. Such a situation, where the non-negligible local truncation error of a numerical scheme recovers correct physical SGS behaviour, is called physically consistent behaviour, see ref. Balsara & Shu (2000); Hickel *et al.* (2006). Apart from the flux-corrected transport (FCT), successfully employed for free shear and wallbounded flows, see ref. Fureby & Grinstein (2002), the piecewise parabolic method (PPM), the multidimensional positive definite advection transport algorithm (MPDATA) method, see ref. Smolarkiewicz & Margolin (1998); Domaradzki *et al.* (2003) as well as weighted essentially non-oscillatory (WENO) Balsara & Shu (2000) schemes have been proposed for implicit LES, see ref. Grinstein & Fureby (2006); Grinstein *et al.* (2007); Thornber *et al.* (2007). Adams *et al.* (2004) and Hickel *et al.* (2006) have developed the adaptive lo-

cal deconvolution method (ALDM) as the first physically consistent ILES model. The ALDM has been applied to a wide range of compressible and incompressible turbulent flows, see ref. Meyer *et al.* (2010); Hickel & Adams (2007); Remmler & Hickel (2012).

The laminar-turbulent transition and first stage of turbulent decay of low to mid Reynolds number Taylor-Green vortices (TGV) has been used to validate and assess the capabilities of these models. In ref. Hu *et al.* (2010) and Hu (2011) the WENO-CU6-M1 model has been proposed as an alternative model for implicit LES of compressible flows. In this work we employ this novel model for the study of low to very high Reynolds number TGV flows in a weakly compressible setting. We therefore validate its physical consistency at low to mid Reynolds numbers, i.e. $Re \leq 3000$ by quantitative comparison to DNS data of Brachet *et al.* and assess the performance for these Re to explicit LES as well as implicit LES with ALDM. In the second part we explore the evolution of the TGV at very high Reynolds number until very long times.

2 Model formulation

2.1 Artificial compressibility approach

At Mach numbers $M \ll 1$ compressibility is negligible, i.e.: $\beta = \frac{1}{\rho} \frac{\partial \rho}{\partial p} \approx 0$. The *artificial compressibility* approach of Chorin (1997) and Temam (1968) assumes a nonzero but constant compressibility for weakly compressible flows. The isentropic compressibility relates to the sound speed by $a^2 = \frac{1}{\rho \beta|_s}$. For flows with $M = 0.1$, as considered within this work $\beta|_s = 0.01$. For isothermal processes $\beta = \beta|_s$ and the ratio of specific heats is $\gamma = 1$. Pressure and density are thus directly related as $p = a^2 \rho$. If a is a sufficiently large constant, density fluctuations can be considered as small.

2.2 Numerical-flux computation adapted to weakly compressible fluid treatment

Within the weakly compressibility approach an energy equation is redundant. Thus, the governing equations of motion are given by the conservation of mass and momentum. In a discrete space-time-domain, the discrete conservation equation $\frac{dU_i}{dt} = -\frac{1}{\Delta x_i} \left(\mathbf{F}(\mathbf{u}(x_{i+\frac{1}{2}}, t)) - \mathbf{F}(\mathbf{u}(x_{i-\frac{1}{2}}, t)) \right)$ for the cell-averaged solution \mathbf{U}_i , where i denotes the cell index, and $\mathbf{u} = (\rho, \rho u)$ the 1-D (for simplicity) solution vector requires approximations for the cell-face fluxes $\mathbf{F}_{i\pm\frac{1}{2}}$. A straightforward low-dissipation flux approximation is due to the Roe (1981) approximate Riemann solver.

Roe's linearization of the local flux Jacobian $\tilde{\mathbf{A}}_j = \tilde{\mathbf{A}}(\hat{u}_L, \hat{u}_R)$ is essential. The eigenvalues of $\tilde{\mathbf{A}}_j$ are $\tilde{\lambda}_j(\hat{u}_L, \hat{u}_R)$ and its right eigenvectors $\tilde{\mathbf{K}}^{(j)}(\hat{u}_L, \hat{u}_R)$ are determined so that the Roe numerical flux function can be computed as:

$$\hat{\mathbf{F}}_{i+\frac{1}{2}} = \frac{1}{2} (\hat{f}_L + \hat{f}_R) - \frac{1}{2} \sum_{j=1}^m \tilde{\alpha}_j |\tilde{\lambda}_j| \tilde{\mathbf{K}}^{(j)} \quad (1)$$

The Roe averaged density $\tilde{\rho}$ and velocity \tilde{u} are obtained from the left and right reconstructed states $\hat{\mathbf{u}}_L$ and $\hat{\mathbf{u}}_R$ as

$$\tilde{\rho} = \sqrt{\rho_L \rho_R}, \quad \tilde{u} = \frac{\sqrt{\rho_L} u_L + \sqrt{\rho_R} u_R}{\sqrt{\rho_L} + \sqrt{\rho_R}}. \quad (2)$$

Within the weakly compressible approach the Roe-averaged speed of sound $\tilde{a} = a$, hence constant. Thus, the eigenvalues $\tilde{\lambda}_j$, the right eigenvectors $\tilde{\mathbf{K}}^{(j)}$ and the wave speeds $\tilde{\alpha}_j$ are:

$$\begin{aligned} \tilde{\lambda}_1 &= \tilde{u} - a, & \tilde{\lambda}_2 &= \tilde{u} + a, \\ \tilde{\mathbf{K}}^{(1)} &= \begin{bmatrix} 1 \\ \tilde{u} - a \end{bmatrix}, & \tilde{\mathbf{K}}^{(2)} &= \begin{bmatrix} 1 \\ \tilde{u} + a \end{bmatrix}, \\ \tilde{\alpha}_1 &= \frac{1}{2\tilde{a}^2} [(p_R - p_L) - \tilde{\rho} a (\hat{u}_R - \hat{u}_L)], \\ \tilde{\alpha}_2 &= \frac{1}{2\tilde{a}^2} [(p_R - p_L) + \tilde{\rho} a (\hat{u}_R - \hat{u}_L)]. \end{aligned} \quad (3)$$

A three-step TVD Runge-Kutta scheme is used for time integration, see Shu (2003).

2.3 Reconstruction of non-averaged states

The smooth densities $\hat{\rho}_L = \hat{\rho}_R$ are reconstructed with a 6^{th} order central scheme. The non-averaged velocities $(\hat{u}, \hat{v}, \hat{w})_{L,R}$ are reconstructed with the 6^{th} order adaptive central-upwind weighted essentially non-oscillatory scale-separation scheme *WENO-CU6-M1* originally proposed for the implicit LES of compressible flows, ref. Hu (2011). For the physically consistent simulation of incompressible isotropic turbulent flows, the modified weights of *WENO-CU6-M1* have been adapted to a linear-weight bias $C_q = 16000$ and a power exponent of $q = 8$.

3 Underresolved numerical simulations of the incompressible three-dimensional Taylor-Green vortex at finite Reynolds numbers

Simulations of the three-dimensional Taylor-Green vortex (TGV) G. I. Taylor (1937) evolving from the initial two-dimensional condition

$$\begin{aligned} u(x, y, z, 0) &= \sin(x) \cos(y) \cos(z), \\ v(x, y, z, 0) &= -\cos(x) \sin(y) \cos(z), \\ w(x, y, z, 0) &= 0, \quad \rho(x, y, z, 0) = 1.0, \\ p(x, y, z, 0) &= 100 + \frac{1}{16} [(\cos(2x) + \cos(2y)) \\ &\quad (2 + \cos(2z)) - 2]. \end{aligned} \quad (4)$$

are conducted within a domain of periodic boundary conditions of $(2\pi)^3$, discretized with a coarse grid of 64^3 cells. To assess resolution effects a refined grid of 128^3 cells is used for $Re \geq 800$. The DNS data of Brachet *et al.* for $Re \leq 3000$ serves as validation data, M.E. Brachet (1984); Brachet *et al.* (1992). The time evolution of the total dissipation rate $\varepsilon = \frac{dE}{dt}$ within $0 < t < 10$ is used for comparison.

Figure 1 depicts the dissipation rates for LES with a conventional ($C_s = 0.18$) and dynamic Smagorinsky model as well as for WENO-CU6-M1-based ILES. The Smagorinsky model with constant C_s overpredicts dissipation even for the smallest $Re = 100$. For larger Reynolds numbers the predictions are unphysical. The dynamic adjustment of the Smagorinsky parameter improves the dissipation rate predictions significantly. For $Re \leq 200$ the agreement with DNS is good. For $Re \geq 400$, the dynamic Smagorinsky model, however, overestimates dissipation rates at early stages, leading to divergence of the solution within time.

With advancing laminar-turbulent transition, the dissipation rate increases due to non-linear vortex stretching.

The decrease in $\varepsilon(t)$ at later stages is due to viscous damping. For Reynolds numbers below $Re = 800$, the dissipation rates obtained with the underresolved WENO-CU6-M1 ILES on the coarse grid are in good agreement with DNS. For $Re \geq 800$ equally good agreement is observed with DNS on the fine grid.

Comparative results are obtained with the adaptive local deconvolution model (ALDM) Hickel *et al.* (2006) for $Re \leq 1600$. At higher Reynolds numbers ALDM, however, overpredicts small scale structures and thus the dissipation rate, whereas the WENO-CU6-M1 scheme underpredicts these, see figure 1e. An almost matching dissipation rate is observed at $Re = 3000$ for the ALDM implicit LES, the WENO-CU6-M1 ILES on the fine grid and the the DNS.

4 Evolution of the incompressible three-dimensional Taylor-Green vortex at very high Reynolds number over long times

On basis of the validation simulations of finite Re TGV evolution to a quasi-isotropic state at $t \approx 9$, see ref. D. Fauconnier (2009), the evolution of the incompressible TGV at physical infinite Reynolds number is studied in detail for an extended time.

The resolved energy spectrum for $0 \leq t \leq 10$ is shown in figure 2a. It evolves from a single characteristic Fourier mode of $E(k=1) = 0.125$ to the entire range of resolvable scales ($k \in [1, 32]$), whereas at $t \approx 3.4$ subgrid-scales are produced and kinetic energy is decayed due to SGS dissipation. For times $9 \leq t \leq 11$ $E \propto t^{-1.3}$ is identified, see figure 2b.

For $11 \leq t \leq 30$ $E(t)$ compares to $t^{-1.6}$ and for times later than $t \approx 30$, $E(t)$ scales according to $t^{-2.6}$, see figure 3. At $t \approx 100$, the self-preserving turbulent decay mechanism is stalling. For these late stages, $E(t) \propto t^{-2}$ is identified.

Following the spectral energy decomposition until $t = 200$, the loss of energy is well observable, see figure 4. However, $E(k)$ compares to $k^{-5/3}$ (dashed lines) at least until $t \approx 70$. For $t \geq 100$ the bandwidth of the inertial subrange narrows progressively. At $t = 200$ only the band within $k = 2$ and $k = 9$ shows Kolmogorov scaling. Higher modes scale according to $E(k) \propto k^{-7/3}$

For the temporal evolution of 3-D isotropic turbulent decay we identify two scaling ranges:

1. $E_1(k, t) \propto k^{-5/3} 1.6^{-(t/10)}$ for $10 \leq t \leq 80$.
2. $E_2(k, t) \propto k^{-5/3} 1.3^{-(t-60)/20}$ is observed for later times ($t \geq 80$).

Low-mode transition to isotropy

For $10 \leq t \leq 30$ redistribution of kinetic energy among the large scale structures is a characteristic indicator of high- Re TGV transition to isotropy, see Fig. 5. We have been able to capture the low-mode transition of the $Re = \infty$ and $Re = 3000$ TGV with our weakly compressible ILES solver on grids of 64^3 and 128^3 (not shown) cells.

During the redistribution of kinetic energy inertial subrange scaling is lost temporarily, compare $E - k$ -plot for $t = 20$. The second mode has temporal minima of the kinetic energy at $t \approx 10$ and $t \approx 18$. At the initiation of this low-mode transition which coincides with the first temporal minima, an overall inter-modal kinetic energy redistribution starts, equalizing the 3-D energy spectrum. Subsequent to the low-mode transition, kinetic energy is well-distributed

within the entire wavenumber spectrum and the $E - k$ -distribution resembles an isotropic Kolmogorov-spectra henceforth.

5 Discussion and Conclusion

In an underresolved setting the weakly compressible WENO-CU6-M1 based ILES perform superior to mathematically more complex explicit LES for a wide range of Reynolds numbers. At higher Reynolds numbers the numerical viscosity is overpredicted by the explicit SGS models to an extent that eventually the introduced numerical viscosity determines the evolution of the flow entirely. At equal resolution the numerically complex ALDM is computationally more expensive than WENO-CU6-M1 implicit LES. Increasing one level of refinement enables to predict dissipation rates comparative to DNS at uncompetitively low costs. Even for the highest finite Reynolds numbers for which DNS data is available, physically consistent TGV evolution is accurately predicted.

The SGS model is inherent in the high-order formulation of the underlying flux computation scheme. With the WENO-CU6-M1 model it can and has been shaped such that the SGS smoothly attach to the resolved scales and thereby emulates the SGS dissipation physically consistently. The resolved scales serve as the model input. Certainty in the model output, the subgrid scales, is ensured when most certain input is provided. Thus, a spatially high-order numerical reconstruction of the unaveraged cell face solutions is required.

The assumed final quasi-isotropic state reached at $t \approx 9$ has been found to be temporary at least for high and infinite Reynolds number Taylor-Green vortices. Our weakly compressible WENO-CU6-M1-based ILES approach allows for self-similar isotropic turbulence to develop properly from laminar-turbulent transition. Two temporal minima within the second mode indicate the onset and seizure of a transitional period approximately. Inertial subrange scaling ($E(k) \propto k^{-5/3}$) is lost temporarily due to redistribution of kinetic energy within the low modes. Analogous transition is observable in the time evolution of the 3-D energy spectra for a Reynolds number of 3000 depicted in ref. Fauconnier *et al.* (2013). The author left this observation undiscussed.

For isotropic turbulence at very high Reynolds numbers the total kinetic energy scales with $t^{-1.2}$, see ref. Marcel Lesieur (2000). Within the quasi-isotropic period $9 \leq t \leq 11$ as well as the isotropic period $30 \lesssim t \lesssim 100$ $E(t)$ has been found to be slightly faster.

Concluding, the proposed conservative weakly compressible WENO-CU6-M1 Roe-Pike method has allowed to explore the very-underresolved incompressible Taylor-Green vortex up to physically infinite Reynolds numbers until the final stage of turbulent decay physically consistently.

Acknowledgements

The authors wish to thank the Deutsche Forschungsgemeinschaft (DFG) for funding. F.S.S. expresses his gratitude to the Hanns-Seidel-Foundation (HSS). We also thank Dr. S. Hickel for the contribution of reference data.

REFERENCES

- Adams, N.A., Hickel, S. & Franz, S. 2004 Implicit subgrid-scale modeling by adaptive deconvolution. *Journal of Computational Physics* **200** (2), 412–431.
- Balsara, Dinshaw S. & Shu, Chi-Wang 2000 Monotonicity preserving weighted essentially non-oscillatory schemes with increasingly high order of accuracy. *Journal of Computational Physics* **160** (2), 405 – 452.
- Brachet, M., Meneguzzi, M., Vincent, A., Politano, H. & Sulem, P.-L. 1992 Numerical evidence of smooth self-similar dynamics and possibility of subsequent collapse for three-dimensional ideal flow. *Physics of Fluids* **4**, 2845–2854.
- Chorin, Alexandre Joel 1997 A numerical method for solving incompressible viscous flow problems. *Journal of Computational Physics* **135**, 118 – 125.
- D. Fauconnier, C. De Langhe, E. Dick 2009 Construction of explicit and implicit dynamic finite difference schemes and application to the large-eddy simulation of the Taylor-Green vortex. *Journal of Computational Physics* **228**, 8053–8084.
- Domaradzki, Julian A., Xiao, Z. & Smolarkiewicz, P.K. 2003 Effective eddy viscosities in implicit large eddy simulations of turbulent flows. *Physics Fluids* **15**, 3890–3893.
- Fauconnier, Dieter, Bogey, Christophe & Dick, Erik 2013 On the performance of relaxation filtering for large-eddy simulation. *JOURNAL OF TURBULENCE* **14** (1), 22–49.
- Fureby, Christer & Grinstein, Fernando F. 2002 Large eddy simulation of high-Reynolds-number free and wall-bounded flows. *Journal of Computational Physics* **181** (1), 68 – 97.
- G. I. Taylor, A.E. Green 1937 Mechanism of the production of small eddies from larger ones. *Proc. R. Soc. Lond. A* **158**, 499–521.
- Grinstein, F.F., Margolin, L.G. & Rider, W. 2007 *Implicit Large Eddy Simulation: Computing Turbulent Fluid Dynamics*. Cambridge Univ Pr.
- Grinstein, Fernando F. & Fureby, Christer 2006 Recent progress on flux-limiting based implicit large eddy simulation. In *European Conference on Computational Fluid Dynamics, ECCOMAS CFD*.
- Hickel, S., Adams, N.A. & Domaradzki, J.A. 2006 An adaptive local deconvolution method for implicit LES. *Journal of Computational Physics* **213** (1), 413–436.
- Hickel, S. & Adams, N. A. 2007 On implicit subgrid-scale modeling in wall-bounded flows. *Physics of Fluids* **19** (10), 105106–105113.
- Hu, X. Y., Adams N. A. 2011 Scale separation for implicit large eddy simulation. *Journal of Computational Physics* **230**, 7240–7249.
- Hu, X. Y., Wang, Q. & Adams, Nikolaus Andreas 2010 An adaptive central-upwind weighted essentially non-oscillatory scheme. *Journal of Computational Physics* **229**, 8952–8965.
- J. Smagorinsky 1963 General circulation experiments with the primitive equations. *Mon. Wea. Rev.* **91** (3), 99–164.
- Marcel Lesieur, Sepand Ossia 2000 3d isotropic turbulence at very high Reynolds numbers: Edqnm study. *Journal of Turbulence* **1**, 1–25.
- Margolin, Len G. & Rider, William J. 2002 A rationale for implicit turbulence modelling. *International Journal for Numerical Methods in Fluids* **39** (9), 821–841.
- M.E. Brachet, D. Meiron, S. Orszag B. Nickel R. Morf U. Frisch 1984 The Taylor-Green vortex and fully developed turbulence. *Journal of Statistical Physics* **34**, 1049 – 1063.
- Meyer, M., Hickel, S. & Adams, N.A. 2010 Assessment of implicit large-eddy simulation with a conservative immersed interface method for turbulent cylinder flow. *International Journal of Heat and Fluid Flow* **31** (3), 368 – 377, sixth International Symposium on Turbulence and Shear Flow Phenomena.
- Remmler, Sebastian & Hickel, Stefan 2012 Spectral structure of stratified turbulence: direct numerical simulations and predictions by large eddy simulation. *Theoretical and Computational Fluid Dynamics* pp. 1–18, 10.1007/s00162-012-0259-9.
- Roe, P. L. 1981 Approximate Riemann solvers, parameter vectors, and difference schemes. *Journal of Computational Physics* **43**, 357–372.
- Sagaut, P. 2005 *Large Eddy Simulation for Incompressible Flows*, 3rd edn. Springer Berlin / Heidelberg.
- Shu, Chi-Wang 2003 High-order finite difference and finite volume WENO schemes and discontinuous Galerkin methods for CFD. *International Journal of Computational Fluid Dynamics* **17** (2), 107–118.
- Smolarkiewicz, Piotr K. & Margolin, Len G. 1998 Mpdata: A finite-difference solver for geophysical flows. *Journal of Computational Physics* **140** (2), 459 – 480.
- Temam, Roger 1968 Une méthode d'approximation des solutions des équations Navier-Stokes. *Bull. Soc. Math.* **98**, 115 – 152.
- Thornber, Ben, Mosedale, Andrew & Drikakis, Dimitris 2007 On the implicit large eddy simulations of homogeneous decaying turbulence. *Journal of Computational Physics* **226** (2), 1902 – 1929.

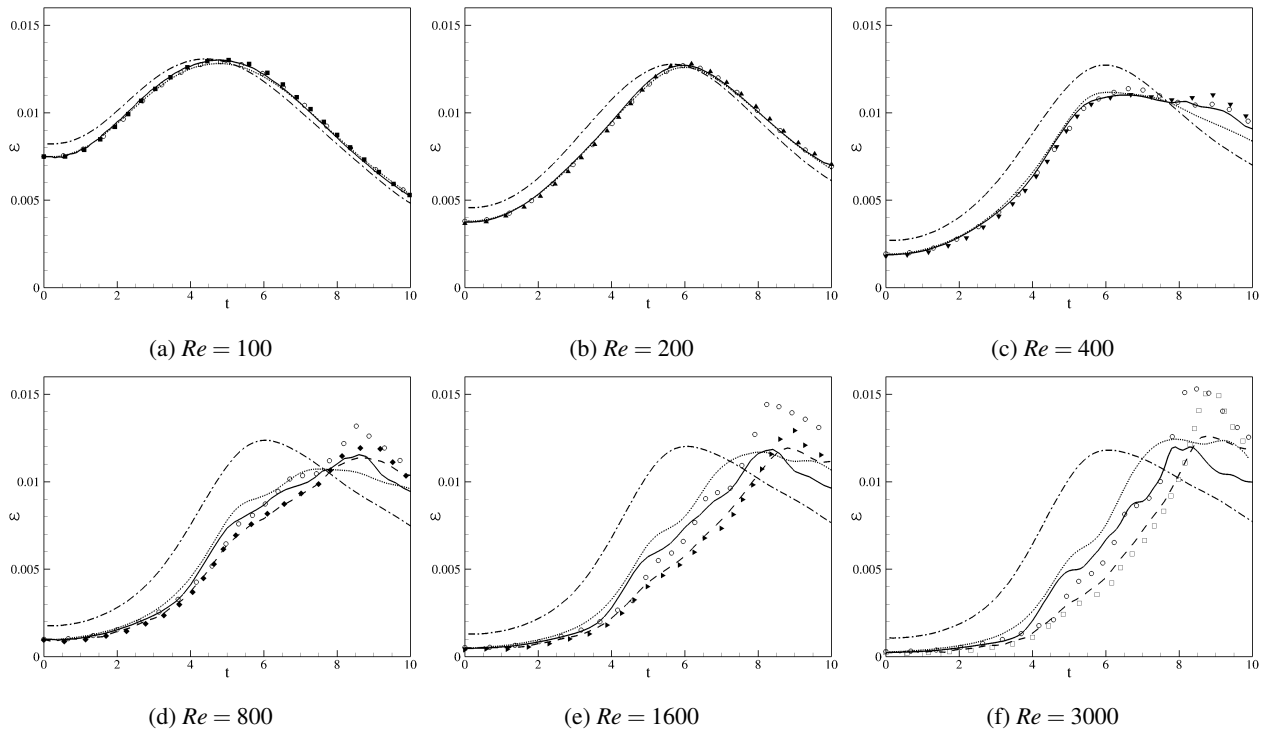


Figure 1: Re specific dissipation rate $\varepsilon(t)$ for the 3-D TGV. With 64^3 cells: — WENO-CU6-M1 implicit LES, - - - constant- C_s Smagorinsky LES, dynamic Smagorinsky LES. On 128^3 FV for $Re \geq 800$: - - - WENO-CU6-M1 ILES. Implicit LES with ALDM Hickel *et al.* (2006) on 64^3 cells: \circ . DNS data by Brachet *et al.*: \blacksquare : $Re = 100$, \blacktriangle : $Re = 200$, \blacktriangledown : $Re = 400$, \blacklozenge : $Re = 800$, \blacktriangleright : $Re = 1600$, \square : $Re = 3000$.

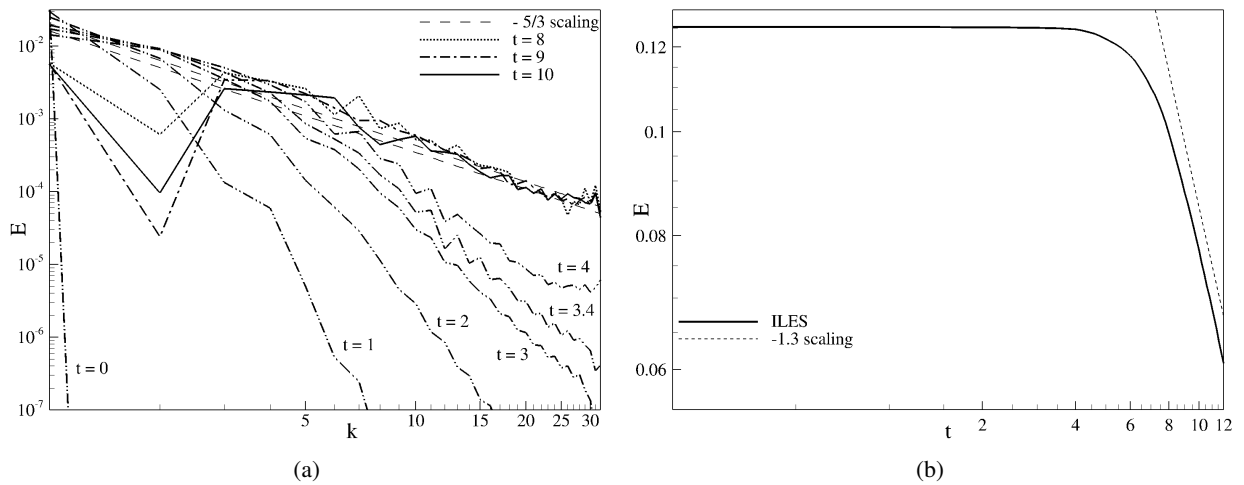


Figure 2: Evolution of the kinetic energy for the early stages ($t \leq 10$) of the inviscid, incompressible Taylor-Green vortex. (a): spectral decomposition of kinetic energy, (b): total kinetic energy.

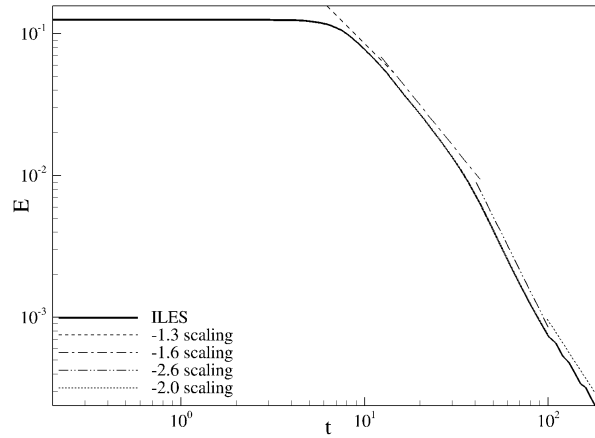


Figure 3: Time evolution of the kinetic energy of the 3-D Taylor-Green vortex ($E-t$) for $t \leq 200$ as compared to idealized scaling of $t^{-1.3}$ for $9 \leq t \leq 11$, $t^{-1.6}$ for $11 \leq t \leq 30$, $t^{-2.6}$ for $30 \leq t \leq 100$, $t^{-2.0}$ for $t \geq 100$

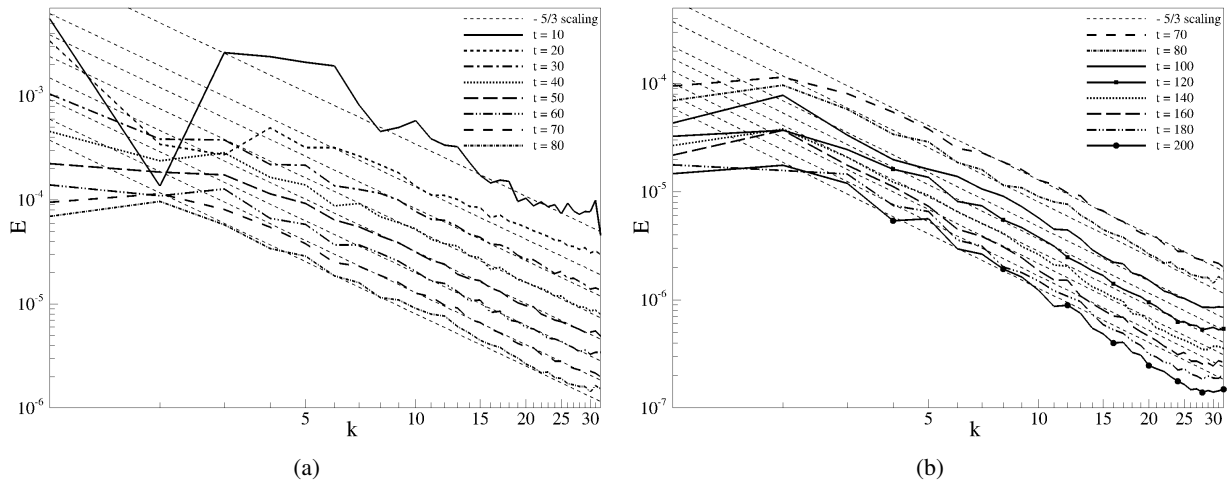


Figure 4: 3-D energy spectrum within resolved inertial subrange compared to Kolmogorov scaling $E(k) \propto k^{-5/3}$.

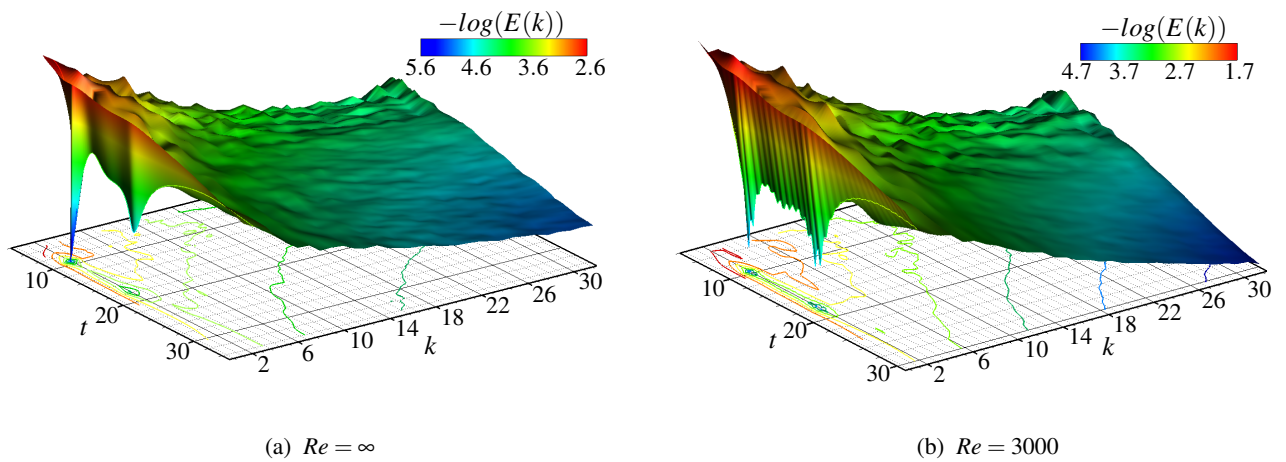


Figure 5: Spectral decomposition of energy (logarithmic scale) for the 3-D TGV ILES within $5 \leq t \leq 35$. Projected contours on $t-k$ -plane are in increments of $10^{0.5}$ for 10^{-6} to 10^{-2} .